



ORIGINAL ARTICLE

Quantitative correlation between counterion (X) binding affinity to cationic micelles and X – Induced micellar growth for substituted iodobenzoates (X)



Nor Saadah M. Yusof, M. Naquiddin M. Said, M. Niyaz Khan *

Department of Chemistry, Faculty of Science, University of Malaya, 50603 Kuala Lumpur, Malaysia

Received 30 October 2012; accepted 21 October 2013

Available online 28 October 2013

KEYWORDS

Rheometric measurements;
Counterion micellar binding;
Substituted iodobenzoates;
Kinetics;
Piperidine;
Phenyl salicylate

Abstract A new semi-empirical kinetic (SEK) method has been used to calculate the values of K_X^{Br} or R_X^{Br} (X represents substituted iodobenzoates), with K_X and K_{Br} representing CTABr micellar binding constants of counterions X^- (in the presence of either spherical or non-spherical micelles) and Br^- (in the presence of only spherical micelles), respectively. Steady-shear rheological properties of mixed 0.015 M CTABr/[MX] aqueous solutions reveal the presence of flexible wormlike micelles where MX represents sodium 3- and 4-iodobenzoates. The maxima of the plots of viscosity vs. [MX] at 0.015 M CTABr for MX representing sodium 3- and 4-iodobenzoates support the presence of long linear and entangled wormlike micelles.

© 2013 King Saud University. Production and hosting by Elsevier B.V. This is an open access article under the CC BY-NC-ND license (<http://creativecommons.org/licenses/by-nc-nd/3.0/>).

1. Introduction

A recent review (Jungwirth and Tobias, 2006) highlights that specific ion effects on aqueous interfaces are ubiquitous both in physical and chemical processes occurring in almost all branches of life and apparent non-life sciences. Kunz et al. (2004) have pointed out that although Hofmeister effects, also known as specific ion effects, are universal in biology (Thirumalai et al., 2012), biochemistry (Berkowitz and Vacha, 2012)

and chemical engineering, for over a hundred years, Hofmeister effects have not been encompassed by theories of solution or colloid chemistry. Similarly, Romsted (2007) has pointed out that the forces contributing to specific ion effects are difficult to identify, both experimentally and theoretically.

It has been known for the last nearly 4 decades that the structural features of counterions play a crucial and important role in the ionic micellar structural transition from spherical to threadlike to flexible entangled wormlike micelles (Magid, 1998; Abdel-Rahem, 2008; Rao et al., 1987; Lin et al., 1994). Qualitative experimental observations on ionic micellar head-group interaction with counterions (X) show that strong ionic micellar binding of counterions results in such micellar structural transition (Lu et al., 1998; Bijma and Engberts, 1997; Ali et al., 2009). Even the recent such studies lacked the quantification of X affinity to ionic micelles and consequently a quantitative correlation between X affinity to micelles and X-induced micellar growth could not be found in these studies

* Corresponding author. Tel.: +60 3 7967 4163; fax: +60 3 7967 4193.

E-mail address: niyaz@um.edu.my (M.N. Khan).

Peer review under responsibility of King Saud University.



Production and hosting by Elsevier

(Ketner et al., 2007; Lin et al., 2009a,b; Sreejith et al., 2011). The competitive binding affinities of X to ionic micelles have been studied because of their importance in the kinetic data analysis of ionic micellar-mediated semi-ionic bimolecular reactions (Bunton, 2006), industrial processes (Qi and Zakin, 2002) and separation science (Trone et al., 2000).

The quantification of counterion (X) binding efficiency with ionic micelles may be achieved in terms of the magnitudes of either the degree of counterion binding (β_X) or usual ion exchange constant (K_X^{Br}) or R_X^{Br} with $R_X^{\text{Br}} = K_X/K_{\text{Br}}$ where the values of cationic micellar binding constants K_{Br} and K_X have been derived from the physicochemical parameters obtained in the presence of spherical and non-spherical micelles, respectively (Khan, 2006). However, the values of β_X for X representing benzoate ions (Wang et al., 2010) as well as 2-, 3- and 4- CH_3Bz^- (where $\text{Bz}^- = \text{C}_6\text{H}_4\text{CO}_2^-$) of cationic micelles are nearly same (Vermathen et al., 2002) but their effects on cationic micellar growth are not the same (Rehage and Hoffmann, 1991). The reported values of K_X^{Br} or R_X^{Br} for X = 3- and 4- CH_3Bz^- are nearly 3-fold larger than that for 2- CH_3Bz^- (Khan and Kun, 2001; Khan and Ismail, 2007). In view of these reports, the values of K_X^{Br} or R_X^{Br} seem to correlate better than those of β_X with X-induced micellar structural growth for different moderately hydrophobic X. But, it is not easy to determine accurately K_X^{Br} because the magnitudes of K_X^{Br} are very much technique-dependent (Magid et al., 1997; Romsted, 1984). A search of the literature reveals a very limited number of the reported values of ion exchange constants with X representing moderately hydrophobic counterions, obtained in the presence of cationic micelles (Magid et al., 1997; Gamboa et al., 1989; Bachofer and Simonis, 1996). A new semi-empirical kinetic (SEK) method has been used to determine the values of K_X^{Br} or R_X^{Br} for X representing both moderately hydrophilic and hydrophobic counterions (Khan, 2006). The effects of the inert counterionic salts on the rates of some ionic micellar-mediated reactions have been quantitatively explained in terms of pseudophase ion exchange (PIE) model (Romsted, 1984). The chemical trapping method of Romsted has been used to determine the value of K_X^{Cl} as 2.6 for X = Br^- (Romsted, 2007) which is similar to ones determined by various methods including the SEK method (Khan and Sinasamy, 2011).

A search of the literature reveals that the values of K_X^{Br} or R_X^{Br} for X = 2-, 3- and 4- IBz^- are unknown. In the continuation of our study (Yusof and Khan, 2010, 2011) on the use of the SEK method for the determination of K_X^{Br} or R_X^{Br} for various X, the present manuscript reports the results for X = 2-, 3- and 4- IBz^- . The aims of the present study were (i) to determine the values of K_X^{Br} or R_X^{Br} for MX = 2-, 3- and 4- IBzNa at different total concentrations of CTABr, (ii) to carry out the rheometric measurements on mixed aqueous solutions of CTABr and MX (MX = 2-, 3- and 4- IBzNa) and (iii) to discover a possible quantitative correlation between the values of K_X^{Br} or R_X^{Br} and X-induced micellar growth. The quantitative correlation between the values of K_X^{Br} or R_X^{Br} and X-induced micellar growth has a predictive strength in the sense that the values of K_X^{Br} or R_X^{Br} can predict whether the X-induced micellar structure is spherical, rodlike/wormlike micelles or even unilamellar vesicles at a constant concentration of CTABr within its range 0.005–0.015 M. The observed results and their probable explanations are described in this manuscript.

2. Experimental

2.1. Materials

Chemicals such as cetyltrimethylammonium bromide (CTABr; purity $\geq 99\%$ from Fluka), phenyl salicylate (PSaH; purity $\geq 98\%$ from Fluka), piperidine (Pip; purity $\geq 99\%$ from Merck), 2-, 3- and 4- IBzH with BzH representing $\text{C}_6\text{H}_4\text{CO}_2\text{H}$ (2- IBzH ; purity $\geq 99\%$ from Merck, 3- IBzH ; purity 98% from Aldrich and 4- IBzH ; purity $\geq 98\%$ from Merck) and NaOH (purity $\geq 99\%$ from Merck) were commercial products with highest available purity. The details of the preparation of the stock solutions of organic salts (MX = 2-, 3- and 4- IBzNa) and PSaH were the same as described earlier (Yusof and Khan, 2011). Because of the extremely low water solubility of PSaH, the stock solutions (0.01 M) of PSaH were prepared in pure acetonitrile.

2.2. Kinetic measurements

The rate of reaction between piperidine (Pip) and ionized phenyl salicylate (PSa^-) was studied spectrophotometrically by monitoring the disappearance of PSa^- as a function of reaction time (t) at a constant wavelength of 350 nm by using UV-visible spectrophotometer equipped with electronically controlled thermostatic cell compartment set at 35 °C. The details of the kinetic procedure and product characterization study were the same as described elsewhere (Khan and Kun, 2001). Nonlinear least-squares technique was used to calculate kinetic parameters k_{obs} (pseudo first-order rate constant), δ_{ap} (apparent molar absorptivity of the reaction mixture) and A_{∞} (absorbance at $t = \infty$) from Eq. (1) (Khan and Kun 2001).

$$A_{\text{ob}} = [\text{R}_0]\delta_{\text{ap}}\exp(-k_{\text{obs}}t) + A_{\infty} \quad (1)$$

where A_{ob} is the absorbance at any reaction time (t) and $[\text{R}_0]$ is the initial concentration of PSaH. Almost all the kinetic runs were carried out for the reaction period equivalent to ~ 9 half lives of the reaction.

2.3. Rheometric measurements

The rheological study was carried out using a Brookfield R/S+ rheometer with double gap coaxial cylinder (CC-DG) and an external temperature controller fixed at 35 °C. The concentrations of all additives except CTABr of a rheological sample were same as maintained in the kinetic measurements. The concentration of CTABr was kept constant at 0.015 M. The sample was thermally equilibrated at 35 °C for at least 15 minutes. The shear rate ($\dot{\gamma}$) range was fixed at 0.5–15 s^{-1} and 1–1000 s^{-1} for respectively the total time of 2400 s and 8000 s, for the rheological measurements. The total number of data points was 30 for the first set and 100 for the second set.

2.4. Determination of K_X^{Br} or R_X^{Br} for X = 2-, 3- and 4- IBz^- by the use of SEK method

The semi-empirical kinetic (SEK) method for the determination of K_X^{Br} or R_X^{Br} requires the use of a reaction kinetic probe which involves the kinetic study on the effects of the

concentrations of the inert salts of counterions (such as [MX] where MX = 2-, 3- and 4-IBzNa) on k_{obs} for the cationic micelle-catalyzed semi-ionic bimolecular reaction with the ionic reactant representing as the counterion of cationic micelle. The reaction kinetic probe that has been used in the present study, involves the nucleophilic reaction of Pip with PSa^- . The details of the SEK method including the reaction kinetic probe used in the present study are described in a recent report (Yusof and Khan, 2010; Khan, 2010).

3. Results

3.1. Effects of the concentrations of 2-, 3- and 4-IBzNa ($\text{Bz}^- = \text{C}_6\text{H}_4\text{CO}_2^-$) on the rate of piperidinolysis of PSa^- at a constant $[\text{CTABr}]_{\text{T}}$ and 35 °C

Several kinetic runs were carried out at different concentrations of MX (= 2-, 3- and 4-IBzNa) within [MX] range 0.0 – ≤ 0.30 M at 0.005 M CTABr, 0.1 M Pip and 2×10^{-4} M PSa^- . The values of [NaOH], under such conditions, varied from 0.03 to 0.06 M for 2-IBzNa and 0.03 to 0.04 M for 3- and 4-IBzNa. The values of pseudo-first-order rate constants (k_{obs}), at different [MX] are shown graphically in Fig. 1 for MX = 3-IBzNa and Figs. S1 and S2 of Supplementary Data (SD) for respective MX = 2 and 4-IBzNa. Similar observations were obtained at 0.006, 0.007, 0.01 and 0.015 M CTABr for MX = 2-IBzNa while for 3- and 4-IBzNa, the observed data could be obtained only at ≤ 0.01 M CTABr. The values of k_{obs} at different [MX] and at a constant 0.015 M CTABr, for MX = 3- and 4-IBzNa could not be obtained because the reaction mixture, even at the lowest value of [MX] (= 0.002 M), became jelly at the reaction time $t = 0$. As a consequence, the reaction mixtures under such conditions became highly viscous and inhomogeneous as well as observed data, A_{obs} vs. t , did not fit to Eq. (1). The

values of k_{obs} at different [MX] and $[\text{CTABr}]_{\text{T}}$ are also shown graphically in Fig. 1, S1 and S2 for MX = 3-, 2- and 4-IBzNa, respectively.

3.2. Effects of [MX] (MX = 2-, 3- and 4-IBzNa) on k_{obs} for the reaction of Pip with PSa^- in the absence of CTABr at 35 °C

Although benzoate and substituted benzoate ions are nonreactive toward nucleophilic cleavage of PSa^- , these inert salts might affect rate of piperidinolysis of PSa^- through specific salt/ionic strength effect. In order to find out this probable salt effect on k_{obs} , a few kinetic runs were carried out at 0.1 M Pip, 2×10^{-4} M PSa^- and within [MX] (MX = 2-, 3- and 4-IBzNa) range 0.0–0.3 M in the absence of CTABr. The values of [NaOH] varied within its range 0.03–0.06 M. The least-squares calculated values of kinetic parameters, k_{obs} and δ_{ap} reveal that the values of k_{obs} are almost independent of [MX] within its range 0.0–0.2 M for MX = 2-IBzNa, 0.0 – 0.10 M for MX = 3- and 4-IBzNa. Mean values of k_{obs} (i.e., $k_{\text{obs}}^{\text{mean}}$) are $(316 \pm 13) \times 10^{-4}$, $(323 \pm 10) \times 10^{-4}$ and $(311 \pm 14) \times 10^{-4} \text{ s}^{-1}$ for MX = 2-, 3- and 4-IBzNa, respectively. The value of k_{obs} at 0.3 M 2-IBzNa is $\sim 10\%$ lower than the mean value of k_{obs} (= $(316 \pm 13) \times 10^{-4} \text{ s}^{-1}$). The values of δ_{ap} remain independent of [MX] within its range 0.0 – 0.3 M and mean values of δ_{ap} (i.e., $\delta_{\text{ap}}^{\text{mean}}$) are 6866 ± 106 , 6769 ± 107 and $6871 \pm 178 \text{ M}^{-1} \text{ cm}^{-1}$ for MX = 2-, 3- and 4-IBzNa, respectively.

3.3. Rheological properties of CTABr micellar solutions containing constant concentrations of PSa^- , Pip, MX and > 0.03 to ≤ 0.04 M NaOH

Rheological behaviors of CTABr/2-IBzNa, CTABr/3-IBzNa and CTABr/4-IBzNa were studied at 33.9 ± 1.6 °C under

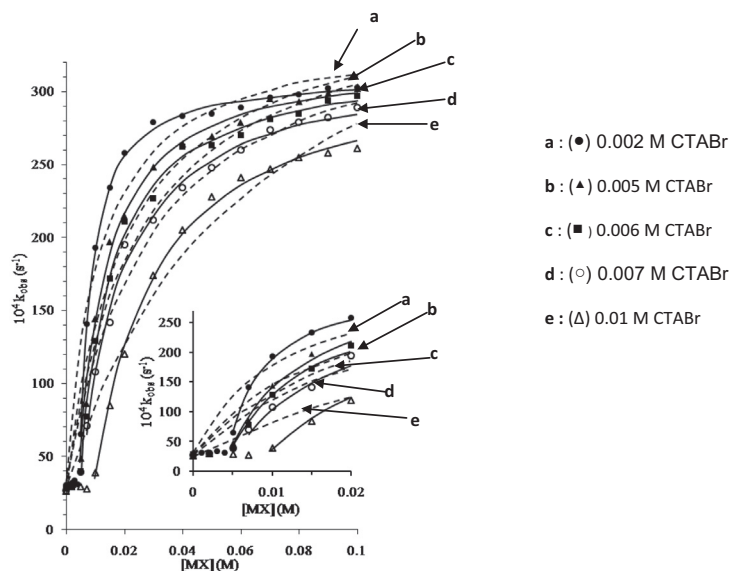


Figure 1 Plots showing the dependence of k_{obs} upon [MX] (MX = 3-IBzNa) for piperidinolysis of PSa^- at 2×10^{-4} M PSa^- , 0.1 M Pip, ≤ 0.06 to > 0.03 M NaOH, 35 °C and $[\text{CTABr}]_{\text{T}}/\text{M} = 0.002$ (●), 0.005 (▲), 0.006 (■), 0.007 (○) and 0.01 (Δ). The dashed lines are drawn through the calculated data points using Eq. (2) with kinetic parameters (k_0 , θ and $\text{K}^{\text{X/S}}$), listed in Table 1 of manuscript, at $[\text{MX}]_0^{\text{op}} = 0$. The solid lines are drawn through the calculated data points using Eq. (2) with kinetic parameters (k_0 , θ and $\text{K}^{\text{X/S}}$), listed in Table 1 of manuscript, at $[\text{MX}]_0^{\text{op}}/\text{M} = 0.0044$ (●), 0.0045 (▲), 0.0046 (■), 0.0050 (○) and 0.0094 (Δ). Inset: The plots at magnified scale for the data points at the lowest values of [MX].

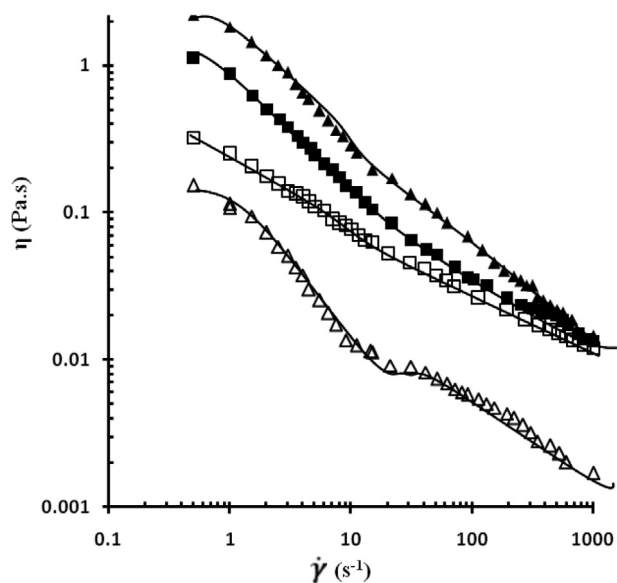


Figure 2 Plots showing the dependence of shear viscosity (η) upon shear rate ($\dot{\gamma}$) for samples where $[\text{PSaH}] = 2 \times 10^{-4}$ M, $[\text{NaOH}] = 0.03$ M, $[\text{Pip}] = 0.1$ M, $[\text{CTABr}] = 0.015$ M and $[\text{3-IBzNa}]/\text{M} = 0.01$ (Δ), 0.03 (\blacktriangle), 0.05 (\blacksquare) and 0.1 (\square).

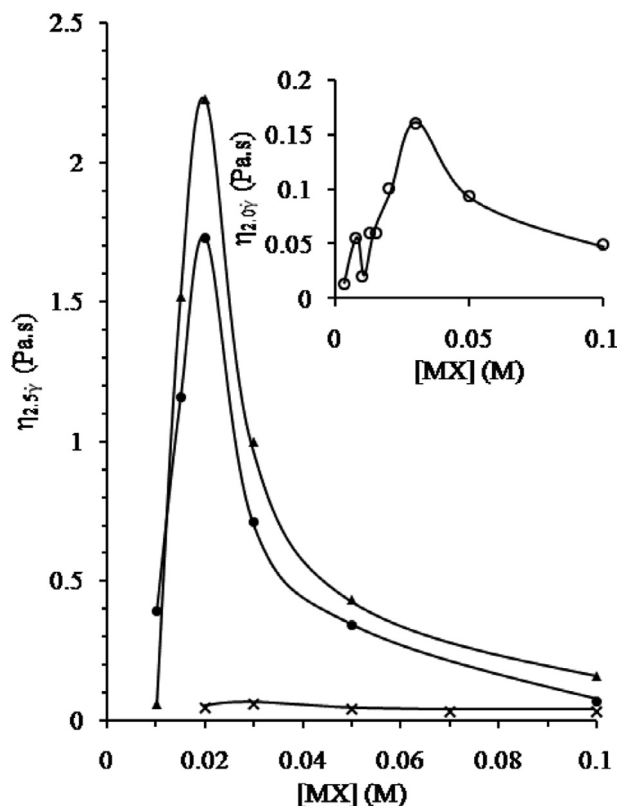


Figure 3 Plot of shear viscosity (η) at $\dot{\gamma} = 2.5 \text{ s}^{-1}$ vs. $[\text{MX}]$ ($[\text{MX}] = [2\text{-IBzNa}]$ (\times), $[3\text{-IBzNa}]$ (\blacktriangle) and $[4\text{-IBzNa}]$ (\bullet)) at 0.015 M CTABr as well as the plot of η at $\dot{\gamma} = 2.0 \text{ s}^{-1}$ vs. $[\text{MX}]$ ($\text{MX} = 4\text{-IBzNa}$) (\circ) at 0.005 M CTABr, 2×10^{-4} M PSa^- , 0.03 M NaOH and 0.1 M Pip and ~ 35 °C.

steady-shear rheological response. Aqueous surfactant (CTABr) solutions containing 2% v/v CH_3CN and a constant concentration of all additives (2×10^{-4} M PSa^- , 0.1 M Pip, ≤ 0.06 M NaOH) including 0.015 M CTABr as well as different concentrations of MX (= 2-, 3- and 4-IBzNa) were used to obtain shear viscosity (η) at different shear rates ($\dot{\gamma}$) within its range $> 0.4 - 1000 \text{ s}^{-1}$. The log-log plots of η vs. $\dot{\gamma}$ at different values of $[\text{MX}]$ are shown graphically by Fig. 2 for MX = 3-IBzNa and respective Figs. S3 and S4 of (SD) for MX = 2- and 4-IBzNa. Similar observations were also obtained at 0.005 M CTABr for 4-IBzNa simply for comparison purpose because the values of η , at shear rates 10 and 1000 s^{-1} and within $[\text{4-IBzNa}]$ range $0.003 - 0.02$ M at 0.005 M CTABr and 30 °C, are available from a recent report (Ge et al., 2008). The values of η vs. $\dot{\gamma}$ are shown graphically as log-log plots in Fig. S5. The plots of Fig. 2 and Figs. S3–S5 represent shear thinning which is a typical characteristic of the presence of rodlike micelles (RM)/wormlike micelles (WM) in the surfactant solutions (Lin et al., 2009a; Lin et al., 2009a; Lu et al., 2008; Raghavan and Kaler, 2001).

The values of η at $\dot{\gamma} = 2.5 \text{ s}^{-1}$, i.e. $\eta_{2.5\dot{\gamma}}$, 0.015 M CTABr and different $[\text{MX}]$ are shown graphically in Fig. 3 for MX = 2-, 3- and 4-IBzNa. The plot of $\eta_{2.0\dot{\gamma}}$ vs. $[\text{4-IBzNa}]$ at 0.005 M CTABr is also shown in Fig. 3. A remarkable rheological feature of adding salt (MX) to aqueous surfactant solutions is the maximum shown by the plot of $\eta_{\dot{\gamma}}$ vs. $[\text{MX}]$. Although this behavior is no longer unusual for long wormlike micellar systems (Rehage and Hoffmann, 1991; Schubert et al., 2004; Croce et al., 2005; Ali and Makhloufi, 1997; Davies et al., 2006), the mechanism, at the molecular level for the occurrence of such maximum, is still a matter of debate (Davies et al., 2006; Dreiss, 2007).

4. Discussion

4.1. Determination of K_X^{Br} or R_X^{Br} for $X = 2\text{-}, 3\text{-}$ and 4-IBz^-

It is evident from Fig. 1 and Figs. S1 and S2 that the values of k_{obs} are more than 10-fold smaller at $[\text{MX}] = 0$ and $[\text{CTABr}]_{\text{T}} \neq 0$ than those at $[\text{CTABr}]_{\text{T}} = 0$, and at different $[\text{MX}]$ within its range $0 - \leq 0.2$ M. Thus, the nonlinear increase in k_{obs} with the increasing values of $[\text{MX}]$ at a constant $[\text{CTABr}]_{\text{T}}$ cannot be explained in terms of ionic strength effect. The most plausible cause for the nonlinear increase in k_{obs} with the increase of $[\text{MX}]$ is the transfer of micellized PSa^- (i.e., PSa^-_{M} with subscript 'M' indicating micellar pseudophase) to the bulk water phase (i.e., PSa^-_{W} with subscript 'W' indicating water phase) through the ion exchange process X^-/PSa^- . The values of k_{obs} , at different $[\text{MX}]$ (MX = 2-, 3- and 4-IBzNa) and at a constant $[\text{CTABr}]_{\text{T}}$, were treated with Eq. (2) (Khan and Ismail, 2007; Khan, 2010).

$$k_{\text{obs}} = \frac{k_0 + \theta K^{X/S} [\text{MX}]}{1 + K^{X/S} [\text{MX}]} \quad (2)$$

where θ and $K^{X/S}$ are empirical constants and $k_0 = k_{\text{obs}}$ at $[\text{MX}] = 0$ as well as $[\text{D}_n] \neq 0$ (where D_n represents micellized CTABr). The nonlinear least-squares technique was used to calculate θ and $K^{X/S}$ as well as least squares, Σdi^2 , (where $\text{di} = k_{\text{obs } i} - k_{\text{calc } i}$ with $k_{\text{obs } i}$ and $k_{\text{calc } i}$ representing respective experimentally determined and least-squares calculated rate constants, at the i -th value of $[\text{MX}]$), from Eq. (2) by

considering k_0 as the known parameter determined experimentally at $[MX] = 0$. The calculated values of θ , $K^{X/S}$ and Σdi^2 at different $[CTABr]_T$ for $MX = 2$ -, 3- and 4-IBzNa are shown in Table 1.

The plots of Fig. 1 as well as Figs. S1 and S2, where dashed lines are drawn through the least squares calculated rate constants using Eq. (2) with kinetic parameters (θ and $K^{X/S}$) listed in Table 1, reveal significant systematic negative deviations of the observed data points from dashed lines at the lower values of $[MX]$. The reason for these significant negative deviations of the observed data points from the corresponding calculated data points with the decreasing $[MX]$ at its extreme lower values as well as higher values of $[CTABr]_T$ has been attributed to the significant effects of the ion exchange processes X^-/HO^- and X^-/Br^- on k_{obs} under such typical reaction conditions (Khan and Ismail, 2007; Yusof and Khan, 2010; Khan, 2010). The consideration of these independent ion exchange processes has led to Eq. (3) (Khan and Ismail, 2007; Khan, 2010)

$$[MX]_S^{ef} = [MX] - [MX]_0^{op} \quad (3)$$

where $[MX]_S^{ef}$ represents the effective concentration of MX that could affect the ion exchange X^-/S^- ($S^- = PSa^-$) and $[MX]_0^{op}$ is the optimum value of $[MX]$ at which the value of $([HO^-_M] + [Br^-_M])$ becomes independent of $[MX]$. The values of $[MX]_0^{op}$ at different values of $[CTABr]_T$ were estimated by an iterative technique (Yusof and Khan, 2010; Khan, 2010). These calculated values of $[MX]_0^{op}$ are summarized in Table 1. The values of θ , $K^{X/S}$ and Σdi^2 were also calculated from Eq. (2) with $[MX] = [MX]_S^{ef}$ and these results are also shown in Table 1. It is evident from the plots of Fig. 1 as well as Figs. S1 and S2, (where solid lines are drawn through the calculated data points using Eq. (2) and kinetic parameters, θ and $K^{X/S}$), with $[MX] = [MX]_S^{ef}$ as well as from the values of Σdi^2 that the observed data treatment with Eq. (2) is more reliable with $[MX] = [MX]_S^{ef}$ at $[MX]_0^{op} \neq 0$ compared with that at $[MX]_0^{op} = 0$.

Table 1 Values of the empirical constants θ and $K^{X/S}$, calculated from Eq. (2) (where $[MX] = [MX]_S^{ef}$ with zero and nonzero $[MX]_0^{op}$ values) for different MX in CTABr micelles.^a

| $[CTABr]_T^b$ (mM) | $10^4 k_0^c$ (s ⁻¹) | $[MX]_{0op}$ (mM) | $10^4 \theta$ (s ⁻¹) | $K^{X/S}$ (M ⁻¹) | $K_{X/S}$ (M ⁻¹) | $F_{X/S}$ | $K_{X/S}^n$ (M ⁻¹) | R_X^{Br} | $10^8 (\Sigma di^2)$ |
|---|---------------------------------|-------------------|----------------------------------|------------------------------|------------------------------|-------------------|--------------------------------|-------------------|----------------------|
| <i>MX = 2-IC₆H₄CO₂Na</i> | | | | | | | | | |
| 5.0 | 29.3 | 4.5 | 254 ± 2.4 ^d | 9.78 ± 0.24 ^d | 352 ^e | 0.78 ^f | 275 ^g | 11.0 ^h | 13.21 |
| 5.0 | 29.3 | 0 | 274 ± 12 | 7.56 ± 0.75 | 272 | 0.84 | 228 | 9.12 | 210.4 |
| 6.0 | 28.8 | 5.6 | 261 ± 6.5 | 8.51 ± 0.52 | 366 | 0.80 | 293 | 11.8 | 66.11 |
| 6.0 | 28.8 | 0 | 286 ± 16 | 6.39 ± 0.82 | 275 | 0.87 | 239 | 9.56 | 272.9 |
| 7.0 | 27.9 | 7.8 | 246 ± 7.3 | 7.96 ± 0.57 | 398 | 0.75 | 299 | 12.0 | 62.90 |
| 7.0 | 27.9 | 0 | 278 ± 22 | 5.49 ± 0.89 | 275 | 0.85 | 234 | 9.36 | 286.4 |
| 10.0 | 27.1 | 9.7 | 229 ± 8 | 5.88 ± 0.45 | 417 | 0.70 | 292 | 11.7 | 38.30 |
| 10.0 | 27.1 | 0 | 274 ± 32 | 3.72 ± 0.78 | 264 | 0.84 | 222 | 8.88 | 240.0 |
| 15.0 | 26.2 | 14.0 | 220 ± 17 | 3.42 ± 0.44 | 363 | 0.67 | 243 | 9.72 | 9.651 |
| 15.0 | 26.2 | 0 | 587 ± 533 | 0.79 ± 0.84 | 83.7 | 1.80 | 151 | 6.04 | 96.44 |
| <i>MX = 3-IC₆H₄CO₂Na</i> | | | | | | | | | |
| 2.0 | 30.5 | 4.4 | 313 ± 1.4 | 247 ± 7.36 | 3705 | 0.96 | 3557 | 142.3 | 90.03 |
| 2.0 | 30.5 | 0 | 344 ± 17 | 90.6 ± 19.2 | 1450 | 1.05 | 1523 | 60.9 | 611.57 |
| 5.0 | 29.5 | 4.5 | 325 ± 3.3 | 112 ± 5.64 | 4032 | 0.99 | 3992 | 159.7 | 26.57 |
| 5.0 | 29.5 | 0 | 368 ± 21 | 49.3 ± 9.61 | 1775 | 1.13 | 2006 | 80.2 | 463.8 |
| 6.0 | 28.4 | 4.6 | 322 ± 3.9 | 93.1 ± 5.21 | 4003 | 0.98 | 3923 | 156.9 | 30.92 |
| 6.0 | 28.4 | 0 | 371 ± 23 | 41.9 ± 8.45 | 1802 | 1.13 | 2036 | 81.4 | 451.25 |
| 7.0 | 27.1 | 5.0 | 322 ± 5.9 | 72.5 ± 5.46 | 3625 | 0.98 | 3553 | 142.1 | 45.41 |
| 7.0 | 27.1 | 0 | 367 ± 16 | 36.7 ± 5.00 | 1835 | 1.12 | 2055 | 82.2 | 151.2 |
| 10 | 26.2 | 9.4 | 322 ± 6.0 | 48.1 ± 3.11 | 3415 | 0.98 | 3347 | 133.9 | 19.28 |
| 10 | 26.2 | 0 | 433 ± 65 | 16.3 ± 5.26 | 1157 | 1.32 | 1527 | 61.1 | 394.7 |
| <i>MX = 4-IC₆H₄CO₂Na</i> | | | | | | | | | |
| 5.0 | 30.9 | 4.4 | 293 ± 2.4 | 115 ± 4.0 | 4140 | 0.90 | 3726 | 149 | 72.38 |
| 5.0 | 30.9 | 0 | 335 ± 25 | 51.2 ± 11 | 1843 | 1.02 | 1880 | 75.2 | 3452 |
| 6.0 | 29.3 | 4.8 | 284 ± 5.0 | 105 ± 7.6 | 4515 | 0.87 | 3928 | 157 | 278.9 |
| 6.0 | 29.3 | 0 | 333 ± 31 | 44.0 ± 12 | 1892 | 1.02 | 1930 | 77.2 | 4373 |
| 7.0 | 27.2 | 5.5 | 289 ± 8.5 | 78.4 ± 8.3 | 3920 | 0.88 | 3450 | 138 | 500.0 |
| 7.0 | 27.2 | 0 | 333 ± 30 | 37.3 ± 9.0 | 1865 | 1.02 | 1902 | 76.1 | 2746 |
| 10.0 | 26.2 | 9.4 | 262 ± 0.2 | 56.1 ± 0.1 | 3983 | 0.80 | 3186 | 127 | 0.075 |
| 10.0 | 26.2 | 0 | 361 ± 30 | 37.2 ± 9.0 | 2641 | 1.10 | 2905 | 116 | 2380 |

^a $[MX] = 2$ -IBzNa, 3-IBzNa and 4-IBzNa.

^b Total concentration of CTABr.

^c $k_0 = k_{obs}$ at $[MX] = 0$.

^d Error limits are standard deviations.

^e $K_{X/S} = K^{X/S} (1 + K_S^0 [CTABr]_T)$ where $K_S^0 = 7000 \text{ M}^{-1}$.

^f $F_{X/S} = \theta/k_W$ where $k_W = k_{obs}$ at $[CTABr]_T = 0$, $[Pip]_T = 0.1 \text{ M}$ and the value of k_W , under such conditions, is $32.7 \times 10^{-3} \text{ s}^{-1}$ at 35°C .

^g $K_{X/S}^n = F_{X/S} K_{X/S}$.

^h $R_X^{Br} = K_{X/S}^n / K_{Br/S}^n$, where $K_{Br/S}^n = 25 \text{ M}^{-1}$.

Table 2 Mean values of $F_{X/S}$ and K_X^{Br} or R_X^{Br} for different MX in the presence of CTABr micelles.^a

| X | [MX] _o ^{op} | 10 ² $F_{X/S}$ | K_X^{Br} or R_X^{Br} | [MX] _{sc} ^b mM | Micelles' structure |
|---|---------------------------------|------------------------------|-----------------------------------|------------------------------------|---------------------|
| 2-IC ₆ H ₄ CO ₂ ⁻ (2-IBz ⁻) | Nonzero zero | 74 ± 5 ^c 104 ± 43 | 11.2 ± 0.9 ^c 8.6 ± 1.4 | | SR ^d |
| 3-IC ₆ H ₄ CO ₂ ⁻ (3-IBz ⁻) | Nonzero zero | 98 ± 0 115 ± 10 | 147 ± 13 73.2 ± 12 | 20 ^e | WM ^f |
| 4-IC ₆ H ₄ CO ₂ ⁻ (4-IBz ⁻) | Nonzero zero | 86 ± 4 104 ± 4 | 143 ± 13 86 ± 20 | 20 ^e , 30 ^g | WM |
| 3-FC ₆ H ₄ CO ₂ ⁻ | Nonzero | 71 | 12.8 ^h | 70, 70 ^h | WM |
| 4-FC ₆ H ₄ CO ₂ ⁻ | Nonzero | 80 | 13.4 ^h | 70, 80 ^h | WM |
| 2-BrC ₆ H ₄ CO ₂ ⁻ | Nonzero | 63 | 8.8 ⁱ | | SR |
| 3-BrC ₆ H ₄ CO ₂ ⁻ | Nonzero | 92 | 71 ⁱ | 30 ^e | WM |
| 4-BrC ₆ H ₄ CO ₂ ⁻ | Nonzero | 98 | 62 ⁱ | 30 | WM |
| C ₆ H ₅ CO ₂ ⁻ | Zero | 70 | 5.8 ^j | | SM ^{k,l} |

^a Cationic CTABr micelles.

^b The specific concentration of MX for the occurrence of the viscosity maximum of the plot of η_γ vs. [MX].

^c Error limits are standard deviations.

^d SR = short rodlike micelles.

^e At 15 mM CTABr.

^f WM = wormlike micelles.

^g At 5 mM CTABr (the value of [MX]_{sc} corresponds to second maximum of the plot).

^h Ref. (Yusof and Khan, 2010).

ⁱ Ref. (Yusof and Khan, 2011).

^j Ref. (Khan and Ismail, 2010).

^k SM = spherical micelles.

^l Ref. Ali and Makhloufi, 1999.

The effective occurrence of ion exchange process X^-/S^- in the related reaction systems has been found to decrease K_S with the increasing [MX] through an empirical relationship (Khan, 2006)

$$K_s = K_s^0 / (1 + K_{X/S}[MX]) \quad (4)$$

where $K_s^0 = K_s$ at [MX] = 0 (Khan and Ismail, 2010). The magnitude of the empirical constant, $K_{X/S}$, is the measure of the ability of counterion, X^- , to expel another counterion, S^- , from the cationic micellar pseudophase to the aqueous phase through the occurrence of ion exchange process X^-/S^- at the cationic micellar surface. It has been shown in the earlier reports (Khan, 2006; Yusof and Khan, 2010; Khan, 2010) that Eq. (4) and a brief reaction mechanism for CTABr micellar-catalyzed reaction of Pip with PSa^- in terms of pseudophase micellar (PM) model can lead to Eq. (2) with respective θ and $K^{X/S}$ expressed by Eqs. (5) and (6), (Yusof and Khan, 2010; Khan and Sinasamy, 2011) respectively,

$$\theta = F_{X/S} k_W^{MX} [Pip]_T \quad (5)$$

where $k_W^{MX} [Pip]_T = k_{obs}$ obtained at a typical value of [MX], [Pip]_T = 0.1 M and [CTABr]_T = 0 as well as $F_{X/S}$ is an empirical constant whose value, by definition, should vary in the range $>0 \leq 1.0$.

$$K^{X/S} = K_{X/S} / (1 + K_S^0 [CTABr]_T) \quad (6)$$

In view of Eq. (2), the values of θ should be independent of [CTABr]_T. Relatively more reliable calculated values of θ (Table 1) are almost independent of [CTABr]_T for MX = 2-, 3- and 4-IBzNa. Mean values of $F_{X/S}$, calculated from Eq. (5) with $k_W^{MX} [Pip]_T = 32.7 \times 10^{-3} s^{-1}$ at 0.1 M Pip, for X = 2-, 3- and 4-IBz⁻, (Yusof and Khan, 2010) are shown in Table 2.

The values of $K_{X/S}$ at different [CTABr]_T were calculated from Eq. (6) with the reported value of $K_S^0 (= 7 \times 10^3 M^{-1})$ (Khan, 2006). These calculated values of $K_{X/S}$, at different [CTABr]_T for X = 2-, 3- and 4-IBz⁻, are shown in Table 1.

Relatively more reliable values of $K_{X/S}$ are almost independent of [CTABr]_T within its range 0.005–≤0.015 M (Table 1) and this is a requirement for the validity of Eq. (4). It has been concluded in the recent reports (Khan and Ismail, 2007; Khan, 2010) that the normalized $K_{X/S}^n (= F_{X/S} K_{X/S})$ and $K_{Y/S}^n (= F_{Y/S} K_{Y/S})$ values are empirically related to the ratio K_X/K_Y , through the relationship: $R_X^Y = K_X/K_Y = K_{X/S}^n/K_{Y/S}^n$ with $K_X = [X_M]/([X_W][D_n])$ and $K_Y = [Y_M]/([Y_W][D_n])$. The values of $K_{X/S}^n$ (Table 1) and the reported value of $25 M^{-1}$ (Yusof and Khan, 2010) for $K_{Br/S}^n$ (with Br = Y) give the values of K_X^{Br} or R_X^{Br} for X = 2-, 3- and 4-IBz⁻. These results are also shown in Table 1. The mean values of K_X^{Br} or R_X^{Br} , obtained within [CTABr]_T range 0.005–≤0.015 M for X = 2, 3- and 4-IBz⁻, are summarized in Table 2.

Perhaps it is noteworthy that the value of $K_{Br/S}^n (= 25 M^{-1})$ has been derived from kinetic parameters obtained in the presence of spherical CTABr micelles (Khan et al., 2000). But the values of $K_{X/S}^n$ may be obtained, depending upon the structural features of X, in the presence of either spherical or nonspherical micelles. Thus, the value of R_X^{Br} becomes usual/conventional ion exchange constant (K_X^{Br}) if the value of $K_{X/S}^n$ is obtained in the presence of spherical micelles.

The cationic micellar structural transition from spherical to rodlike micelles (RM) and RMs + vesicles is shown to accompany by significant increase in the degree of counterion (X = Br) binding (β_X) (Ono et al., 2005; Rodriguez et al., 2009). However, although β_X values for CTACl/4-XBzNa (with X = F, Cl, Br, I) systems vary only slightly with the change of X from F to I, cryo-TEM images for 0.005 M CTACl/0.003 M MX reveal the presence of only spherical micelles for X = 4-FBz⁻ while mixed spherical + long RM of different natures for X = 4-ClBz⁻, 4-BrBz⁻ and 4-IBz⁻ (Ge et al., 2008). The values of R_X^{Br} for X = 3-ClBz⁻ (Khan and Ismail, 2009), 4-BrBz⁻ (Yusof and Khan, 2011) and 4-IBz⁻ (Table 2) are many folds larger than that for X = 4-FBz⁻ (Yusof and Khan, 2010). Similarly, the values of R_X^{Br} for X = 3-BrBz⁻ and 3-IBz⁻ are larger by respectively 1.4- and

2.8-fold than that for $X = 3\text{-IBz}^-$ (Khan and Ismail, 2009). The increase in electronegativity and polarizability of the substituent of counterions X is expected to decrease and increase the values of K_X^{Br} or R_X^{Br} , respectively. The increase in the steric requirements of X is also expected to possibly decrease the values of K_X^{Br} or R_X^{Br} . Thus, ~ 10 -fold larger value of R_X^{Br} for $X = 4\text{-IBz}^-$ than that for $X = 4\text{-FBz}^-$ may be ascribed to the combined effects of electronegativity, polarizability and steric requirements of F and I.

4.2. Rheological behavior of aqueous solutions of CTABr containing 2-, 3- and 4-IBzNa

Generally, shear viscosity (η) vs. shear rate ($\dot{\gamma}$) plot of worm-like micellar solutions reveals four distinct regions, i.e. Newtonian, shear thinning, shear thickening and shear thinning (Ge et al., 2008). The initial Newtonian regions of Fig. 2 and Figs. S3–S5 (SD) appear to be missing presumably because these Newtonian regions are expected to appear at very low shear rates ($< 0.4 \text{ s}^{-1}$). The rheometer used in this study could not measure the shear viscosity at $\dot{\gamma} < \sim 1.0 \text{ s}^{-1}$ for $\text{MX} = 2\text{-IBzNa}$ and $\dot{\gamma} < \sim 0.4 \text{ s}^{-1}$ for $\text{MX} = 3\text{-}$ and 4-IBzNa at 0.015 M CTABr. Although the plots of Fig. 2 and Figs. S3–S5 do not show the distinct presence of shear thickening regions, most of these plots do indicate regions of very low gradients (within $\dot{\gamma}$ range $\sim 25\text{--}200 \text{ s}^{-1}$, Fig. S3, and $\sim 6\text{--}30 \text{ s}^{-1}$, Fig. 2 and Figs. S4 and S5), between two different shear thinning regions at some values of $[\text{MX}]$. The regions of very low gradients are more apparent with $\text{MX} = 2\text{-IBzNa}$ (Fig. S3) than those with $\text{MX} = 3\text{-}$ and 4-IBzNa (Fig. 2 and Figs. S4 and S5). It is also evident from the plots of Fig. 2 and Figs. S3 and S5 that the plots representing initial shear thinning regions have significantly larger absolute values of gradients for $\text{MX} = 2\text{-IBzNa}$ than those for $\text{MX} = 3\text{-}$ and 4-IBzNa . This may be attributed to the presence of short RM for $\text{MX} = 2\text{-IBzNa}$ and long flexible RM/WM for $\text{MX} = 3\text{-}$ and 4-IBzNa . The flow curve at 0.01 M 2-IBzNa exhibits shear thickening while shear thickening does not exist under essentially similar conditions for $\text{MX} = 3\text{-}$ and 4-IBzNa . Shear thickening, similar to one at 0.01 M 2-IBzNa in Fig. S3, is also exhibited by the flow curve at $[\text{MX}] = 0$ in Fig. S4. It is known from the literature that the aqueous solution containing $< \sim 0.2 \text{ M}$ (Rao et al., 1987) and $< \sim 0.1 \text{ M}$ CTABr (Geng et al., 2005) contains only spherical micelles. Perhaps it is relevant to note that the flow curve at 0.01 M 2-IBzNa (Fig. S3) is very similar to what one would see if Taylor vortices (an unstable flow that occurs in Couette flow of low viscosity fluids at high shear rates) were present. These observations reveal the presence of spherical micelles at 0.01 M 2-IBzNa and RM (rodlike micelles) at 0.01 M MX with $\text{MX} = 3\text{-}$ and 4-IBzNa . Nearly 13-fold smaller value of R_X^{Br} for $X = 2\text{-IBz}^-$ than those for $X = 3\text{-}$ and 4-IBz^- is the most probable cause for the presence of short RM for $\text{MX} = 2\text{-IBzNa}$ and long flexible RM for $\text{MX} = 3\text{-}$ and 4-IBzNa .

It seems noteworthy that the shapes of the flow curves (i.e., the plots of η vs. $\dot{\gamma}$) at different $[\text{MX}]$ for $\text{MX} = 2\text{-}$, 3- and 4-IBzNa are significantly different from the corresponding plots for $\text{MX} = 2\text{-}$, 3- and 4-BrBzNa (Yusof and Khan, 2011) as well as 3- and 4-FBzNa (Yusof and Khan, 2010). The flow curves at 0.01 M MX show the presence and absence of RM for respectively $\text{MX} = 3\text{-IBzNa}$ (Fig. 2) and 3-BrBzNa (Yusof

and Khan, 2011). This distinct difference is attributed to 2-fold larger value of R_X^{Br} for $X = 3\text{-IBz}^-$ than that for $X = 3\text{-BrBz}^-$ (Yusof and Khan, 2011). The characteristic differences between the flow curves for $\text{MX} = \text{FBzNa}$ (Yusof and Khan, 2010), BrBzNa (Yusof and Khan, 2011) and IBzNa may be attributed to significantly large differences in the magnitudes of R_X^{Br} for $X = \text{FBz}^-$, BrBz^- and IBz^- (Table 2).

The presence of two maxima in the plot of $\eta_{2.5\dot{\gamma}}$ vs. $[\text{4-IBzNa}]$ at 0.005 M CTABr (Fig. 3) is comparable with a recent study on rheological behavior of 0.005 M CTACl solutions mixed with $[\text{4-IBzNa}]$ in the range $0.003\text{--}0.02 \text{ M}$ (Ge et al., 2008). However, the plot of $\eta_{2.5\dot{\gamma}}$ vs. $[\text{4-IBzNa}]$ at 0.015 M CTABr exhibits the presence of only one maximum (Fig. 3).

Cryo-TEM image for CTACl/4-IBzNa system at 0.005 M CTACl and 0.02 M 4-IBzNa has long flexible and entangled rodlike micelles (RM) (Ge et al., 2008). Thus, it may not be unreasonable to propose that CTABr/3-IBzNa and CTABr/4-IBzNa systems have long linear and entangled RM at both 0.005 and 0.015 M CTABr. For the CTACl/4-FBzNa system at 0.005 M CTACl and 0.02 M 4-FBzNa , the cryo-TEM image has spherical and some short stiff RM (Ge et al., 2008). The value of R_X^{Br} for $X = 4\text{-FBz}^-$ (Yusof and Khan, 2010) is only slightly larger than that for $X = 2\text{-IBz}^-$ (Table 2). The near similarity of R_X^{Br} values for $X = 2\text{-IBz}^-$ and 4-FBz^- , nearly 13-fold larger value of R_X^{Br} for $X = 4\text{-IBz}^-$ than that for $X = 2\text{-IBz}^-$ and characteristically different natures of the plots of Figs. S3 and S5 may be attributed to the probable presence of short stiff RM in CTABr/2-IBzNa system at 0.015 M CTABr and different concentrations of 2-IBzNa . It is evident from the plots of Fig. 3 that the aqueous solutions of CTABr/MX contain large number of long linear RM even at 0.003 M CTAX ($X = 4\text{-IBz}^-$).

4.3. Relationship between the magnitudes of R_X^{Br} and X-induced micellar growth

Since 1976, the attempts of finding new viscoelastic additives have relied upon the qualitative perception that unusually strong counterionic (X) binding to ionic micelles is the main cause for the X -induced viscoelastic wormlike micellar behavior of aqueous ionic surfactant solutions containing counterionic salts (MX) (Lu et al., 1998; Bijma and Engberts, 1997; Ali et al., 2009; Vermathen et al., 2002; Davies et al., 2006; Gravsholt, 1976; Oelschlaeger et al., 2010; Abezgauz et al., 2010; Takeda et al., 2011; Penfold et al., 2004). Relatively more reliable values of R_X^{Br} for $X = 2\text{-}$, 3- and 4-IBz^- (Table 2) indicate, perhaps for the first time for these counterions (X), a quantitative correlation between the values of R_X^{Br} and X -induced formation of short RM for $X = 2\text{-IBz}^-$ as well as long linear and entangled RM for $X = 3\text{-}$ and 4-IBz^- at the constant $[\text{CTABr}]$ ($= 0.005$ or 0.015 M) and varying values of $[\text{MX}]$. The value of $[\text{MX}]_{\text{sc}}$ represents the specific value of $[\text{MX}]$ at which maximum density of entangled RM occurs at a constant $[\text{CTABr}]$ ($= 0.015 \text{ M}$) in the plot of $\eta_{\dot{\gamma}}$ vs. $[\text{MX}]$. It may be noteworthy that the values of $[\text{MX}]_{\text{sc}}$ remain unchanged with the change of $\dot{\gamma}$ from ~ 2 to 1000 s^{-1} . Thus, if the density of entangled RM formation increases with the increase of the ionic micellar binding constants of counterions (X) at a constant $[\text{CTABr}]$ then the values of $[\text{MX}]_{\text{sc}}$ should decrease with the increase of R_X^{Br} . The listed values of $[\text{MX}]_{\text{sc}}$ vs. R_X^{Br} of Table 2 for $X = 3\text{-}$, 4-FBz^- , 3- , 4-BrBz^- and 3- , 4-IBz^- support this conclusion.

5. Conclusions

(i) The new and perhaps interesting findings of the present study are the experimentally determined values of R_X^{Br} of 11, 147 and 143 for $X = 2-$, $3-$ and $4-IBz^-$, respectively. (ii) One typical advantage of the SEK method is that it gives the values of both K_X^{Br} and R_X^{Br} while all the other existing methods, to the best of our knowledge, can give only the values of K_X^{Br} and not R_X^{Br} . (iii) Rheometric data of this study show the presence of short rigid rodlike micelles for $X = 2-IBz^-$ and long linear and entangled rodlike micelles for $X = 3-$ and $4-IBz^-$. (iv) Here in this article, a quantitative correlation is presented between the values of R_X^{Br} and X-induced micellar structures of short rigid rodlike micelles for $X = 2-IBz^-$ and long linear and entangled RM micelles for $X = 3-$ and $4-IBz^-$ at $[MX]$ range ~ 0.005 or $0.01-0.02$ M in the presence of 0.005 or 0.015 M CTABr. (v) The positions of maxima in the plots of η_{sp} vs. $[MX]$ remain essentially unchanged with the change of $\dot{\gamma}$ within its range 2 to 10^3 s^{-1} . (vi) The kinetic validity of Eq. (3) constitutes an indirect evidence for the occurrence of two or more than two independent ion exchange processes under the present reaction conditions.

Acknowledgements

The authors thank the University of Malaya (UM) for financial assistance through research grant HIR UM/MOHE/SC/07, RG022/09AFR, and the Centre of Ionic Liquids, UM for the permission to carry out the rheological study.

Appendix A. Supplementary data

Supplementary data associated with this article can be found, in the online version, at <http://dx.doi.org/10.1016/j.arabj.2013.10.020>.

References

- Abdel-Rahem, R., 2008. *Adv. Colloid. Interface Sci.* 141, 24 (references cited therein).
- Abezgaus, L., Kuperkar, K., Hassan, P.A., Ramon, O., Bahadur, P., Danino, D., 2010. *J. Colloid Interface Sci.* 342, 83.
- Ali, A.A., Makhloufi, R., 1997. *J. Rheol.* 41, 307.
- Ali, A.A., Makhloufi, R., 1999. *Colloid Polym. Sci.* 277, 270.
- Ali, M., Jha, M., Das, S.K., Saha, K., 2009. *J. Phys. Chem. B* 113, 15563.
- Bachofer, S.J., Simonis, U., 1996. *Langmuir* 12, 1744.
- Berkowitz, M.L., Vacha, R.M., 2012. *Acc. Chem. Res.* 45, 74.
- Bijma, K., Engberts, J.B.F.N., 1997. *Langmuir* 13, 4843.
- Bunton, C.A., 2006. *Adv. Colloid Interface Sci.* 123–126, 333–343.
- Croce, V., Cosgrove, T., Dreiss, C.A., King, S., Maitland, T., Hughes, T., 2005. *Langmuir* 21, 6762.
- Davies, T.S., Ketner, A.M., Raghavan, S.R., 2006. *J. Am. Chem. Soc.* 128, 6669.
- Dreiss, C.A., 2007. *Soft Matter* 3, 956 (and references cited therein).
- Gamboa, C., Rios, H., Sepulveda, L., 1989. *J. Phys. Chem.* 93, 5540.
- Ge, W., Kesselman, E., Talmon, Y., Hart, D.J., Zakin, J.L., 2008. *J. Non Newtonian Fluid Mech.* 154, 1.

- Geng, Y., Romsted, L.S., Froehner, S., Zanette, D., Magid, L.J., Cuccovia, I.M., Chaimovich, H., 2005. *Langmuir* 21, 562.
- Gravsholt, S., 1976. *J. Colloid Interface Sci.* 57, 575.
- Jungwirth, P., Tobias, D., 2006. *Chem. Rev.* 106, 1259.
- Khan, M.N., Arifin, Z., Ismail, E., Ali, S.F.M., 2000. *J. Org. Chem.* 65, 1331.
- Khan, M.N., Kun, S.Y., 2001. *J. Chem. Soc. Perkin Trans. 2*, 325.
- Khan, M.N., 2006. *Surfactant Science Series*, 133. CRC Press, Taylor & Francis Group, Boca Raton, FL (Chapter 3 and references cited therein).
- Khan, M.N., Ismail, E., 2007. *J. Mol. Liq.* 136, 54.
- Khan, M.N., Ismail, E., 2009. *J. Phys. Chem. A* 113, 6484 (and references cited therein).
- Khan, M.N., 2010. *Adv. Colloid Interface Sci.* 159, 160.
- Khan, M.N., Ismail, E.J., 2010. *Dispersion Sci. Technol.* 31, 314.
- Khan, M.N., Sinasamy, S., 2011. *Int. J. Chem. Kinet.* 43, 9.
- Ketner, A.M., Kumar, R., Davies, T.S., Elder, P.W., Raghavan, S.R., 2007. *J. Am. Chem. Soc.* 129, 1553.
- Kunz, K., Henle, J., Ninham, B.W., 2004. *Curr. Opin. Colloid Interface Sci.* 9, 19.
- Lin, Z., Cai, J.J., Scriven, L.E., Davis, H.T., 1994. *J. Phys. Chem.* 98, 5984.
- Lin, Y., Qiao, Y., Yan, Y., Huang, J., 2009a. *Soft Matter* 5, 3047.
- Lin, Y., Han, X., Huang, J., Fu, H., Yu, C., 2009b. *J. Colloid Interface Sci.* 330, 449.
- Lu, B., Zheng, Y., Davis, H.T., Scriven, L.E., Talmon, Y., Zakin, J.L., 1998. *Rheol. Acta* 37, 528.
- Lu, T., Huang, J., Li, Z., Jia, S., Fu, H., 2008. *J. Phys. Chem. B* 112, 2909.
- Magid, L.J., Han, Z., Warr, G.G., Cassidy, M.A., Butler, P.W., Hamilton, W.A., 1997. *J. Phys. Chem. B* 101, 7919.
- Magid, L.J., 1998. *J. Phys. Chem. B* 102, 4064.
- Oelschlaeger, C., Suwita, P., Willenbacher, N., 2010. *Langmuir* 26, 7045.
- Ono, Y., Kawasaki, H., Annaka, M., Maeda, H., 2005. *J. Colloid Interface Sci.* 287, 685.
- Penfold, J., Tucker, L., Staples, E., Thomas, R.K., 2004. *Langmuir* 20, 8054.
- Qi, Y., Zakin, J.L., 2002. *Ind. Eng. Chem. Res.* 41, 6326.
- Raghavan, S.R., Kaler, E.W., 2001. *Langmuir* 17, 300 (and references therein).
- Rao, U.R.K., Manohar, C., Valaulikar, B.S., Iyer, R.M., 1987. *J. Phys. Chem.* 91, 3286.
- Rehage, H., Hoffmann, H., 1991. *Mol. Phys.* 74, 933.
- Rodriguez, A., Graciani, M.M., Cordobes, F., Moya, M.L., 2009. *J. Phys. Chem. B* 113, 7767.
- Romsted, L.S., 1984. In *Surfactant in Solutions*. In: Mittal, K.L., Lindmann, B. (Eds.). Plenum, New York, p. 1015.
- Romsted, R.S., 2007. *Langmuir* 23, 414 (and references cited therein).
- Schubert, B.A., Wagner, N.J., Kaler, E.W., 2004. *Langmuir* 20, 3564.
- Sreejith, L., Parathakkat, S., Nair, S.M., Kumar, S., Varma, G., Hassan, P.A., Talmon, Y., 2011. *J. Phys. Chem. B* 115, 464.
- Takeda, M., Kusano, T., Matsunaga, T., Endo, H., Shibayama, M., Shikata, T., 2011. *Langmuir* 27, 1731.
- Thirumalai, D., Reddy, C., Straub, J.E., 2012. *Acc. Chem. Res.* 45, 83.
- Trone, M.D., Mack, J.P., Goodell, H.P., Khaledi, M.G., 2000. *J. Chromatogr. A* 888, 229.
- Vermathen, M., Stiles, P., Bachofer, S.J., Simonis, U., 2002. *Langmuir* 18, 1030.
- Wang, H., Feng, Q., Wang, J., Zhang, H., 2010. *J. Phys. Chem. B* 114, 1380.
- Yusof, N.S.M., Khan, M.N., 2010. *Langmuir* 26, 10627.
- Yusof, N.S.M., Khan, M.N., 2011. *J. Colloid Interface Sci.* 357, 121.